

# Neutral manganese acceptor in GaP: An electron-paramagnetic-resonance study

J. Kreissl

*Arbeitsgruppe Elektron-Paramagnetische-Resonanz am Institut für Festkörperphysik, Technische Universität Berlin, Rudower Chaussee 5, 12484 Berlin, Germany*

W. Ulrici

*Paul-Drude-Institut für Festkörperelektronik, Hausvogteiplatz 5-7, 10117 Berlin, Germany*

M. El-Metoui, A.-M. Vasson, A. Vasson, and A. Gavaix

*Laboratoire des Sciences et Matériaux pour l'Electronique et d'Automatique, Unité de Recherche Associée au Centre National de la Recherche Scientifique No 1793, Université Blaise Pascal-Clermont-Ferrand II, 63177 Aubière Cedex, France*

(Received 4 December 1995)

In order to clarify the nature of the neutral Mn acceptor in GaP, we have carried out optical-absorption and electron-paramagnetic-resonance (EPR) experiments using both conventional and thermally detected EPR on semi-insulating GaP:Mn. In thermal equilibrium at low temperatures, all the manganese occurs in the charged acceptor state  $\text{Mn}_{\text{Ga}}^{2+}(A^-)$ . By illumination with photon energies greater than 1.2 eV, it can be partially converted into the neutral charge state. The arising photostimulated EPR spectrum shows the characteristic of a tetragonally distorted center with an integer spin. The resonance lines are detectable only at temperatures below 7 K, and their linewidth of about 50 mT is due to the unresolved Mn-hyperfine splitting. We interpret the experimental data in terms of  $\text{Mn}_{\text{Ga}}^{3+}$  ions on strain-stabilized sites of tetragonal symmetry due to a strong  $T \otimes \epsilon$  Jahn-Teller coupling within the  ${}^5T_2$  ground state. Such a behavior is expected for a  $3d^4$  defect, as observed for the isoelectronic impurity  $\text{Cr}^{2+}$  in GaAs, and other tetrahedrally coordinated semiconductors. The analysis of the EPR spectra thus verifies that, in GaP, the neutral charge state of the Mn acceptor is  $\text{Mn}_{\text{Ga}}^{3+}(A^0)$  in contrast to its behavior in GaAs and InP. [S0163-1829(96)06139-5]

## I. INTRODUCTION

Manganese is one of the most intensively investigated transition-metal (TM) impurities in III-V semiconductors. Among its peculiarities are its much higher solubility and diffusivity compared with other  $3d^n$  impurities (except Cu), and that it forms the shallowest of the deep TM single acceptors ( $A^0/A^-$  or  $\text{TM}^{3+}/\text{TM}^{2+}$ ).

The most important problem, debated for a long time, was the description of the electronic ground state of the neutral manganese acceptor. Either the hole is within the  $d$  shell as for all other TM's, so that the neutral acceptor state ( $A^0$ ) is  $\text{Mn}^{3+}$  ( $3d^4$ ), or the hole is bound in a delocalized  $1S_{3/2}$  orbit around the  $\text{Mn}^{2+}$  ( $3d^5$ ) acceptor core (i.e., the neutral Mn acceptor is a  $[\text{Mn}^{2+}, \text{hole}]$  complex).

For GaAs:Mn it is now unequivocally clarified that the second model describes all experimental results consistently. This shallow character has been in evidence from electron-paramagnetic-resonance (EPR) experiments, and confirmed by other techniques. From the similarity of the optical spectra of GaAs:Mn and InP:Mn, it can be expected that the neutral manganese acceptor is also  $\text{Mn}^{2+}$  coupled with a delocalized hole in InP. However, in GaP:Mn, no features which could be related to the neutral Mn have been observed so far. For example, no EPR signal in the usual range of magnetic field in the current experiments at the X band, and no sharp line near the onset of the photoionization band in the optical-absorption spectra of  $p$ -type materials, have been observed in contrast to similar experiments in GaAs:Mn and InP:Mn.

The manganese acceptor level is deeper in GaP than in GaAs and InP. In GaAs, it is indeed the shallowest of the TM levels. If the neutral acceptor is a  $\text{Mn}^{3+}$  deep center, it is expected to give rise to EPR lines similar to those of the isoelectronic  $\text{Cr}^{2+}$  ion ( $3d^4$ ) in GaAs and InP. The aim of this paper is to search for such EPR signals for the GaP:Mn system. After presenting a background on the Mn acceptor in GaAs, InP, and GaP, we study semi-insulating GaP:Mn with the Fermi level above the Mn acceptor level. By illumination at low temperatures, a photostimulated recharging of  $\text{Mn}_{\text{Ga}}^{2+}(A^-)$  is possible, as shown previously for other  $\text{TM}_{\text{Ga}}$  impurities in GaP. This recharging was monitored by optical absorption and particularly by EPR. Another paramagnetic resonance spectrum appears, detected both by conventional EPR and thermally detected (TD) EPR, with an intensity proportional to the photostimulated decrease of the  $\text{Mn}_{\text{Ga}}^{2+}(A^-)$  signal (charged acceptor state). The analysis of this spectrum suggests that it is due to  $\text{Mn}_{\text{Ga}}^{3+}(A^0)$  ( $3d^4$ ) by comparison with that of the isoelectronic  $\text{Cr}^{2+}$  in GaAs, InP, and GaP.

## II. BACKGROUND: MANGANESE IN GaAs, InP, AND GaP

In GaAs:Mn, EPR investigations have shown<sup>1-3</sup> that the isotropic resonance at  $g=2.77$  is the  $\Delta M=\pm 1$  transition within the  $J=1$  ground state resulting from the weakly bound hole ( $j=3/2$ ) exchange coupled to the  $3d^5$  core ( $S=\frac{5}{2}$ ). Also the  $\Delta M=\pm 2$  transition at  $g=5.72$  could be detected. These results have been confirmed by optically detected magnetic resonance (ODMR) via EPR-induced changes in magnetic

circular dichroism (MCD) on  $p$ -GaAs:Mn.<sup>4</sup> Also, the measurements of the temperature dependence of the paramagnetic susceptibility and magnetization could be interpreted consistently within this model,<sup>5</sup> ruling out previous interpretations of such experiments in the framework of the  $3d^4$  model.<sup>6,7</sup> In the first paper concerned with optical absorption of  $p$ -GaAs:Mn, Chapman and Hutchinson<sup>8</sup> observed a broad absorption band (onset at about 0.1 eV, maximum at about 0.2 eV) due to the charge-transfer transition

$$A^0 + h\nu \rightarrow A^- + \text{hole}_{\text{vb}}, \quad (1)$$

in addition to three sharp peaks at its onset. These peaks were assigned to transitions to excited states of a hole weakly bound to the Mn acceptor core. This interpretation has been supported by recent investigations of these peaks by uniaxial stress and Zeeman Fourier-transform absorption spectroscopy.<sup>9,10</sup> The peaks at 101.20, 105.16, 107.07, and 108.05 meV can be assigned to transitions from the ground state ( $1S_{3/2}$ ) to the shallow effective-mass-like excited states  $2P_{3/2}(\Gamma_8)$ ,  $2P_{5/2}(\Gamma_8)$ ,  $2P_{5/2}(\Gamma_7)$ , and  $3P_{5/2}(\Gamma_8)$  of a neutral acceptor, respectively. The optical ionization energy is found to be 112.4 meV.

For  $p$ -InP:Mn the optical-absorption spectrum<sup>11</sup> also showed a broad photoionization band (onset at about 0.20 eV, maximum at about 0.38 eV) due to transition (1), as well as three sharp peaks at 204.6, 210, and 213.1 meV, attributed to the transitions  $1S_{3/2} \rightarrow 2P_{3/2}(\Gamma_8)$ ,  $2P_{5/2}(\Gamma_8)$ , and  $2P_{5/2}(\Gamma_7)$ , respectively, of a weakly bound hole with an optical ionization energy of 220.4 meV. These same energy separations between the  $1S_{3/2}$  and  $2P$  states were also obtained in photoluminescence excitation (PLE) experiments,<sup>12</sup> which revealed additional splittings: the one at 184.6 meV was interpreted as that of the  $1S_{3/2} \rightarrow 2S_{3/2}$  transition, which is forbidden in direct absorption. Thus the neutral manganese acceptor seems also to form a  $[\text{Mn}^{2+}, \text{hole}]$  complex in InP. However, from EPR, ODMR, and optically detected electron-nuclear double-resonance (ODENDOR) experiments,<sup>13-15</sup> no evidence for either a center with a  $J=1$  ground state or for a  $\text{Mn}^{3+}$  ( $3d^4$ ) ion has been found so far. The interpretation of the susceptibility results, presupposing a  $\text{Mn}^{3+}$  ground state,<sup>16</sup> are questionable in the same way as that for the GaAs host.

Manganese in GaP has been investigated in  $n$ - (codoped with shallow donors) and  $p$ -conducting (only Mn or Mn+Zn doping) material. By several independent methods, it was established that Mn forms a single acceptor  $A^0/A^-$  located  $410 \pm 20$  meV above the valence-band edge.<sup>17-19</sup> From EPR and ENDOR experiments on  $n$ -type GaP:Mn, it follows that the ionized acceptor state is the isolated  $\text{Mn}_{\text{Ga}}^{2+}(A^-)$  ( $3d^5$ ) configuration.<sup>20-23</sup> The spin-Hamiltonian parameters derived from the cubic spectrum with six resolved  $^{55}\text{Mn}$  ( $I=\frac{5}{2}$ ) hyperfine lines for the  ${}^6A_1$  ground state are  $g=2.002$ ,  $A=-53.05 \times 10^{-4} \text{ cm}^{-1}$ , and  $a=10 \times 10^{-4} \text{ cm}^{-1}$ . By photoluminescence (PL), the internal  ${}^4T_1 \rightarrow {}^6A_1$  transition of  $\text{Mn}_{\text{Ga}}^{2+}(A^-)$  was detected,<sup>24</sup> and consists of a broad band peaked at about 1.2 eV and a zero-phonon line (zpl) at 1.534 eV followed by several phonon replicas involving an impurity-induced gap mode of  $\hbar\omega=39.5$  meV. This internal PL has been used to investigate the ODMR of sulfur donors.<sup>25</sup> The analysis of uniaxial stress and Zeeman experiments on the 1.534-eV zpl indicated a strong  $T \otimes \epsilon$  Jahn-

Teller coupling on the excited  ${}^4T_1$  state.<sup>26</sup> The internal  ${}^4T_1 \rightarrow {}^6A_1$  transition has also been investigated in manganese-doped  $\text{GaAs}_{1-x}\text{P}_x$  ( $0.25 < x < 1$ ) by PL.<sup>27</sup>

The results available for  $p$ -GaP:Mn are less clear. By optical absorption, a broad photoionization band has also been found (onset at about 0.4 eV, maximum at about 0.8 eV),<sup>17,18,23</sup> and assigned to transition (1). However, no sharp-line structure near the onset of this band has been reported. The EPR results are contradictory. In some cases, in  $p$ -GaP:Mn, the  $\text{Mn}_{\text{Ga}}^{2+}(A^-)$  resonance has been observed.<sup>18,20</sup> In  $p$ -GaP:Mn:Zn,<sup>23</sup> the spectrum of cubic  $\text{Mn}^{2+}$  was absent, and an orthorhombic Mn spectrum with a resolved  $^{55}\text{Mn}$  hyperfine structure ( $|A|=57 \times 10^{-4} \text{ cm}^{-1}$ ) has been detected. This spectrum has been interpreted as arising from Mn on a tetrahedral interstitial site complexed with a nearest-neighbor Ga vacancy. However, the interstitial position of  $\text{Mn}^{2+}$  in this center is questionable, as the hyperfine constant  $A$  is nearly the same as that for substitutional  $\text{Mn}^{2+}$ . Recent EPR and ENDOR experiments on neutron-irradiated GaP [Ref. 28] have suggested that  $\text{Mn}^{2+}$  exists on interstitial sites, and is characterized by a considerably larger hyperfine constant ( $|A|=88.8 \times 10^{-4} \text{ cm}^{-1}$ ) compared with substitutional  $\text{Mn}^{2+}$ . However, the identification of interstitial  $\text{Mn}^{2+}$  is not conclusive. The observation of nearly identical  $\text{Mn}^{2+}$  spectra in different materials<sup>28,29,30</sup> and their powderlike behavior makes it likely that the origin of that spectrum is a  $\text{Mn}^{2+}$  ion at interfaces or at the surface, i.e., Mn is not incorporated in the lattice.

Even though there is no doubt about the existence of a  $\text{Mn}_{\text{Ga}}$  acceptor level  $A^0/A^-$  at  $E_{\text{vb}}+0.41$  eV, no reliable information is available at present to ascribe the neutral state of the manganese acceptor in GaP to a  $\text{Mn}_{\text{Ga}}^{3+}$  ion or a ( $\text{Mn}_{\text{Ga}}^{2+}, \text{hole}$ ) complex.

### III. EXPERIMENTAL DETAILS

The samples investigated were cut from the seed end ( $A1$ ) and from the tail end ( $E1$ ) of a liquid-encapsulated Czochralski (LEC)-grown GaP boule (diameter 40 mm, length 100 mm) doped by adding metallic manganese to the melt. The Mn concentrations determined spectrochemically are  $2 \times 10^{16} \text{ cm}^{-3}$  for the  $A1$  samples, and  $9 \times 10^{16} \text{ cm}^{-3}$  for the  $E1$  samples. Iron is an usual residual impurity in LEC-grown III-V semiconductors. In  $E1$  samples of the GaP:Mn boule, where all Fe is in the  $\text{Fe}^{2+}$  charge state, its content was estimated to be  $[\text{Fe}] \approx 8 \times 10^{14} \text{ cm}^{-3}$  from the  ${}^5E \rightarrow {}^5T_2$  zero-phonon lines in the optical-absorption spectrum using the calibration factor available for  $\text{Fe}^{2+}$  in InP.<sup>31</sup>

Oriented samples have been prepared with dimensions  $12 \times 3 \times 3$  and  $15 \times 5 \times 7 \text{ mm}^3$ , with the long axis parallel to  $\langle 110 \rangle$  for rotation of the magnetic field  $B$  in a  $\{110\}$  plane. A second set of samples with their long axis along  $\langle 100 \rangle$  was prepared for rotation of  $B$  in a  $\{100\}$  plane. Their large faces were polished to carry out both optical-absorption and EPR experiments under additional exciting illumination (photoinduced optical absorption, photo-EPR).

The conventional EPR spectra were measured with a Bruker ESP 300E spectrometer equipped with a gas-flow cryostat. The principles of the technique and the arrangement for thermally detected (TD) EPR at liquid-helium temperatures are described in Ref. 32. Both conventional and TD-

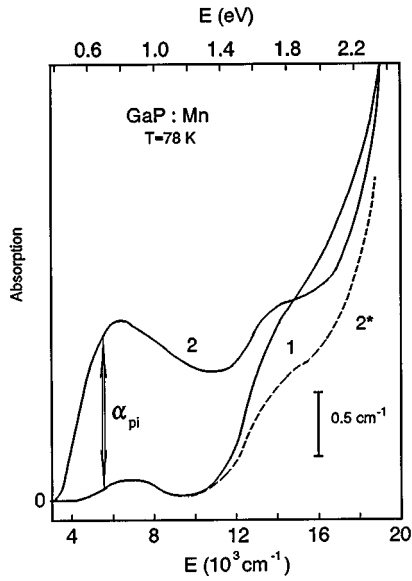


FIG. 1. Optical-absorption spectra of a GaP:Mn *E1* sample measured at  $T=78$  K. Spectrum 1: after cooling in the dark. Spectrum 2: during illumination with  $h\nu_{\text{exc}}=2.0$  eV. Spectrum 2\* (dashed curve) was calculated by subtracting the photoionization absorption due to Eq. (2) from spectrum 2.

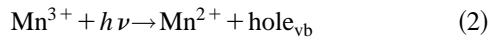
EPR experiments have been carried out at the  $X$  band.

#### IV. RESULTS

##### A. Optical absorption

Curve 1 in Fig. 1 shows the optical-absorption spectrum of a GaP:Mn *E1* sample at 78 K. It consists of a broad photoionizationlike tail with an onset at about 1.2 eV, and two weak broad bands with maxima at 0.87 and 1.75 eV. The band at 1.75 eV is due to the spin-forbidden  ${}^6A_1 \rightarrow {}^4T_1$  transition of  $\text{Mn}_{\text{Ga}}^{2+}(A^-)$ . The corresponding PL spectrum with zpl at 1.534 eV and phonon replicas were also detected at  $T=4.2$  K, in accordance with Ref. 24. The origin of the band at 0.87 eV has not yet been clarified.

Curve 2 of Fig. 1 was obtained during illumination with  $h\nu_{\text{exc}}=2.0$  eV. It is dominated by the appearance of a broad absorption with an onset at 0.4 eV and a maximum at about 0.8 eV. This absorption is due to photostimulated  $\text{Mn}_{\text{Ga}}^{3+}(A^0)$ , as its spectral shape is identical with that of the photoionization transition



detected on heavily Mn-doped  $p$ -type GaP.<sup>17</sup> The amount of photostimulated  $\text{Mn}_{\text{Ga}}^{3+}(A^0)$  is represented by the photostimulated absorption coefficient  $\alpha_{\text{pi}}$  measured at 0.7 eV. Curve 2\* of Fig. 1 was obtained from curve 2 by subtracting the photoionization absorption (2) with a maximum at about 0.8 eV, where its spectral dependence in the region above 1.2 eV was taken from the absorption of  $p$ -GaP:Mn (Ref. 17) fitted to curve 2 in the region 0.4 to 1.2 eV. Curve 2\* demonstrates clearly that the broad photoionization absorption with an onset at 1.2 eV decreases with increasing  $\alpha_{\text{pi}}$ . The same spectra and photostimulated effects were observed on *A1* samples but with smaller  $\alpha_{\text{pi}}$  because of the lower Mn content. Figure 2 shows the spectral dependence of  $\alpha_{\text{pi}}$  which

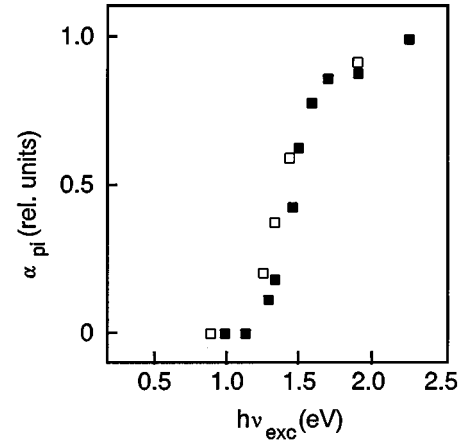
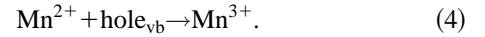


FIG. 2. Dependence of the normalized photostimulated absorption  $\alpha_{\text{pi}}$  (see Fig. 1) on illumination energy  $h\nu_{\text{exc}}$  of GaP:Mn obtained at  $T=78$  K. ■, sample *E1*. □, sample *A1*.

has its onset at 1.2 eV. The comparison of the absorption spectra of Fig. 1 with Fig. 2 suggests the following recharging process. An unidentified defect  $X$  with a level position  $X^0/X^+$  at about  $E_{\text{vb}}+1.2$  eV can be occupied by electrons excited from the valence band according to



and the  $\text{hole}_{\text{vb}}$  are captured by  $\text{Mn}_{\text{Ga}}^{2+}(A^-)$  which exists only in the dark (see below) forming  $\text{Mn}_{\text{Ga}}^{3+}(A^0)$ :



The unidentified defect  $X$  must be a deep donor as all Mn acceptors are compensated; i.e., they are in the  $\text{Mn}_{\text{Ga}}^{2+}(A^-)$  state. For *E1* samples ( $[\text{Mn}]=9 \times 10^{16} \text{ cm}^{-3}$ ) the concentration of  $X$  should be larger than  $8 \times 10^{16} \text{ cm}^{-3}$ . Compensating for the Mn acceptors, a considerable number of the  $X^0/X^+$  levels are emptied and are available for the recharging process (3). A possible candidate for  $X$  would be the phosphorous antisite defect, but its concentration is too low by an order of magnitude (see Sec. III B).

The photostimulated  $\text{Mn}_{\text{Ga}}^{3+}(A^0)$  signal intensity decays very slowly in the dark after switching off the illumination; the decay varies as  $-\ln(t/\tau)$  with  $\tau \approx 10^6$  s. Such a logarithmic decay was found also for other photoinduced  $\text{TM}_{\text{Ga}}$  centers in GaAs and GaP.<sup>35</sup> However, the original situation can be restored optically by illumination with light of energy  $0.4 \text{ eV} < h\nu < 1.2 \text{ eV}$ , i.e., by illumination into the  $\text{Mn}^{2+}/\text{Mn}^{3+}$  photoionization band according to (2). This behavior is illustrated in Fig. 3 for the  $\text{Mn}^{3+}$ -related absorption  $\alpha_{\text{pi}}$ ; it was also monitored for the  $\text{Mn}_{\text{Ga}}^{2+}(A^-)$  resonance signal.

##### B. Conventional EPR

The EPR spectra were investigated in the magnetic field region up to  $B=2.1$  T. In both *E1* and *A1* samples, the well-resolved six-line spectrum due to the negatively charged acceptor  $\text{Mn}_{\text{Ga}}^{2+}(A^-)$  ( $S=\frac{5}{2}$ ) with the same parameters  $g$ ,  $A$ , and  $a$ , as found earlier,<sup>20</sup> dominates the spectra in the low-field region (0–0.5 T, see Fig. 4). The linewidth of the single hyperfine lines is  $\Delta B_{pp} \approx 6$  mT. Additionally, in

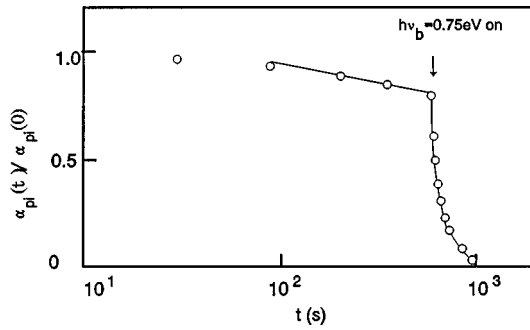


FIG. 3. Decay of the photostimulated  $\text{Mn}_{\text{Ga}}^{3+}(A^0)$  absorption ( $\alpha_{\text{pi}}$  at 0.7 eV) observed at  $T=78$  K in the dark after switching off  $h\nu_{\text{exc}}=2.0$  eV at  $t=0$ , and after switching on the bleaching illumination  $h\nu_b=0.75$  eV at  $t=600$  s.

both kinds of samples the weak resonances due to the antisite defect,  $\text{P}_{\text{Ga}}^{4+}\text{P}_4$ , were found [estimated concentration:  $(5\pm 3)\times 10^{15}$   $\text{cm}^{-3}$ ].

Under illumination with band-gap light, the concentration of  $\text{Mn}_{\text{Ga}}^{2+}(A^-)$  decreases (Fig. 4), and simultaneously a photostimulated spectrum appears (Fig. 5). The large linewidth of about 50 mT suggests that it can be due to a Mn-related center. It is most probable that this large linewidth is caused by an unresolved Mn hyperfine structure which is schematically included in Fig. 5. If the temperature is raised above 7 K, there is a rapid decrease in the observability of the spectrum due to line broadening. The angular dependence for a rotation of the magnetic field in a  $\{100\}$  crystal plane is shown in Fig. 6. It appears to be a typical curve for a tetragonally distorted center with the zero-field splitting of the ground state due to the tetragonal distortion larger than the

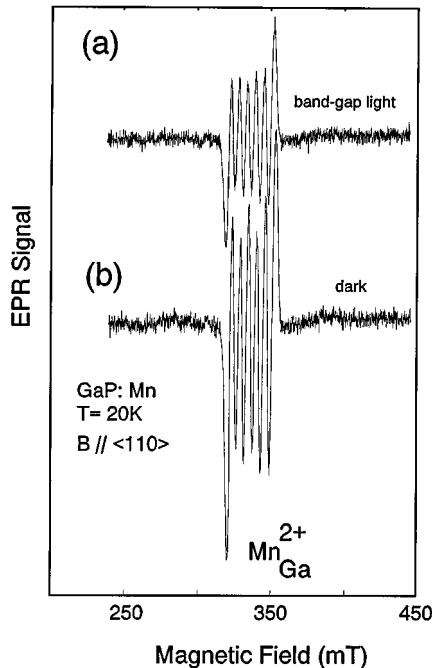


FIG. 4. Conventional EPR spectra of  $\text{Mn}_{\text{Ga}}^{2+}(A^-)$  in GaP at 9.45 GHz with additional band-gap illumination (a) and without illumination (b) at 20 K and the magnetic field oriented along a  $\langle 110 \rangle$  axis.

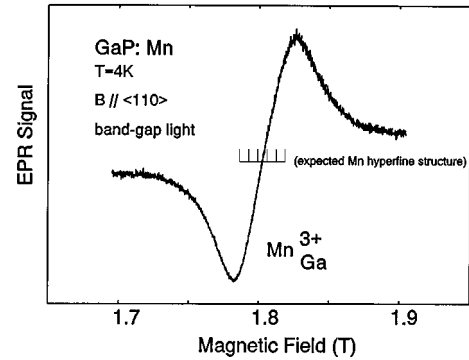


FIG. 5. Conventional photostimulated EPR spectrum of  $\text{Mn}_{\text{Ga}}^{3+}(A^0)$  in GaP at  $T=4$  K and 9.45 GHz, and  $B\parallel\langle 110 \rangle$ . The expected  $^{55}\text{Mn}$  hyperfine structure is included for comparison with the linewidth.

Zeeman splitting as observed by TD EPR for the most intense resonance of  $\text{Cr}^{2+}$  in GaAs,<sup>34</sup>  $\text{InP}$ ,<sup>35</sup> and GaP.<sup>36</sup> In addition to the signals detected at higher magnetic fields, several broad lines were observed in the low-field range which cannot be unambiguously identified as  $\text{Mn}_{\text{Ga}}^{3+}(A^0)$  resonances.

### C. TD EPR

TD EPR is a powerful tool, particularly for the identification of impurities which are strongly coupled to the semiconductor lattice. This is expected to be the situation for the neutral manganese acceptor if it exists as a  $3d^4$  ion in GaP. In the low-field region ( $B=0-0.6$  T), the signals due to  $\text{Mn}_{\text{Ga}}^{2+}(A^-)$ , and the phosphorous antisite  $\text{P}_{\text{Ga}}^{4+}\text{P}_4$  could be detected in the A1 and E1 GaP:Mn samples. Additional signals appear after illumination. However, they cannot be due to a  $3d^4$  ion. Figure 7 shows typical TD EPR spectra in the high-field region (about 1–3 T) for the main directions  $B$  along  $\langle 100 \rangle$  and  $\langle 110 \rangle$  in E1. Before illumination, only weak resonances, unidentified so far, are detected. Following illu-

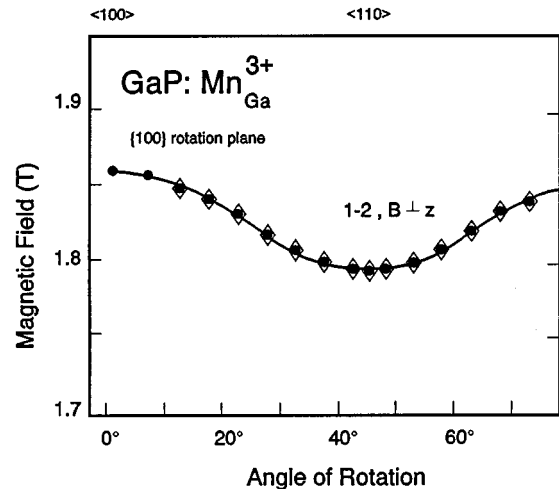


FIG. 6. Angular dependence of the 1-2 fine-structure transition (see Fig. 9) of  $\text{Mn}_{\text{Ga}}^{3+}(A^0)$  measured by EPR ( $\bullet$ ) and TD EPR ( $\diamond$ ) on a GaP:Mn A1 sample. The solid curve is the fit of the data points with the Hamiltonian (5) and the parameters of Table I.

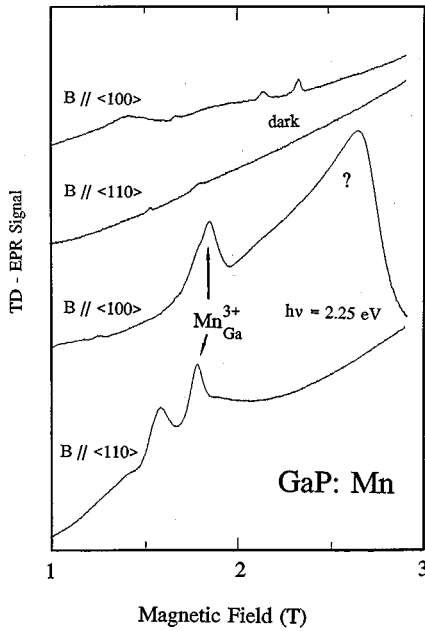


FIG. 7. TD EPR spectra of a GaP:Mn E1 sample observed at  $T=4\text{K}$  with  $B\parallel\langle 100\rangle$  and  $\langle 110\rangle$ . The upper spectra are measured in the dark, and the lower ones after illumination with  $h\nu_{\text{exc}}=2.25\text{eV}$ . The arrows indicate the signal due to the 1-2 transition of  $\text{Mn}_{\text{Ga}}^{3+}(A^0)$ .

mination, additional lines are created. A very broad and intense photostimulated signal appears at  $B=2.7\text{T}$  which is very strongly angular dependent, and can be observed for a few degrees around  $B$  parallel to  $\langle 100\rangle$  only. The assignment of this signal remains unclear.

In the magnetic-field region 1.7–1.9 T, a signal with a linewidth of about 50 mT is detected after illumination in both A1 and E1 samples, also by TD EPR. In E1, it overlaps with other photoinduced lines for some orientations. In A1, it is the only line seen at higher fields. Its angular dependence is identical with that measured by conventional EPR (Fig. 6). This signal has been investigated at different frequencies between 9 and 10 GHz.

## V. DISCUSSION

The photostimulated lines which could be related to Mn are intense in the high-field region. By the fact that the transition probability in the low-field region ( $g_{\text{eff}}$  about 2 and greater than 2) is low, one can conclude that an integer spin system with an even number of unpaired electrons is responsible. These behaviors coincide with the expected properties for a  $3d^4$  system inferring that, in GaP, the neutral Mn acceptor is  $\text{Mn}_{\text{Ga}}^{3+}(A^0)$ . In the following we will analyze the photostimulated spectrum within the assumption of a  $3d^4$  system occupying a  $T_d$  site. The ground state of a  $3d^4$  ion in a tetrahedral field is  ${}^5T_2$ , and the excited state is  ${}^5E$  separated by the crystal-field splitting  $\Delta$ . The  ${}^5T_2$  ground state undergoes a  $T\otimes\epsilon$  Jahn-Teller effect, and is thus split by combined interaction with the spin-orbit coupling, random strains, and any magnetic field which is present. The EPR spectrum is dominated by tetragonally strain-stabilized sites,<sup>37</sup> and thus the size of strains is unimportant provided it is higher than a

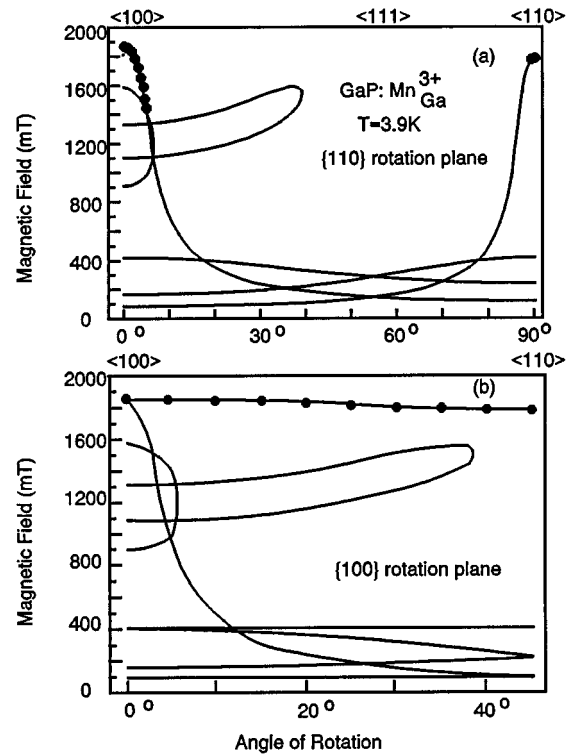


FIG. 8. Angular dependence of the fine-structure line positions of the  $\text{Mn}_{\text{Ga}}^{3+}(A^0)$  charge state in GaP obtained at 9.44 GHz. The magnetic field is rotated in  $\{110\}$  (a) and  $\{100\}$  (b) crystal planes. The experimental data are given by solid circles, and the theoretical fit by solid lines (details concerning the calculation are given in the text).

certain minimum value. The five lowest states from  ${}^5T_2$  can be described by the spin Hamiltonian ( $S=2$ ) (e.g., Ref. 34)

$$\mathcal{H} = g_{\parallel}\mu_B B_z S_z + g_{\perp}\mu_B (B_x S_x + B_y S_y) + D[S_z^2 - \frac{1}{3}S(S+1)] + \frac{1}{6}a(S_x^4 + S_y^4 + S_z^4) + \frac{1}{180}F\{35S_z^4 + [25 - 30S(S+1)]S_z^2\}, \quad (5)$$

where the  $z$  axis of the coordinate system coincides with the cubic  $[001]$  axis, and the  $x$  and  $y$  axes are parallel to  $[100]$  and  $[010]$ , respectively. There are three magnetically different sites. The parameters required to fit the experimental points of the angular dependencies in Figs. 6 and 8 are given in Table I. The intense lines observed experimentally in the high-field region are caused by transitions within the Kramers doublet labeled 1 and 2 in Fig. 9. The solid lines in Fig. 8 are calculated using the parameters of Table I and an exact diagonalization of the spin Hamiltonian (5). The advantage of a rotation in a  $\{100\}$  crystal plane is the much weaker angular dependence connected with an easier observability. However, for the detectable transitions the angular dependencies are extremely sensitive to misalignments of the rotation axis in both the  $\{110\}$  and  $\{100\}$  rotation planes. Therefore, great care was needed during the alignment of the samples in the cryostat for reproducible results. The calculation of transition probabilities through the calculation of the eigenfunctions shows that the largest transition probability is for the so-called 1-2 transition at  $B$  perpendicular to  $z$ . This result supports our observation that the most intense lines

TABLE I. EPR parameter of tetragonally distorted  $3d^4$  centers in GaAs, InP, and GaP. \* assumes  $F=0$ .

Material: center	$g_{\parallel}$	$g_{\perp}$	$D$ ( $\text{cm}^{-1}$ )	$a$ ( $\text{cm}^{-1}$ )	$F$ ( $\text{cm}^{-1}$ )	Method	Ref.
GaAs:Cr	1.974(3)	1.997(2)	$-1.860(16)^*$	$0.031(13)^*$	$0^*$	EPR	39
	-	-	$-1.895(5)$	$0.035(2)$	$-0.053(3)$	TD EPR	34
InP:Cr $^{2+}$	1.981(3)	2.010(5)	$-0.967(1)^*$	$0.089(7)^*$	$0^*$	EPR	40
	1.933	1.968	$-0.97$	0.114	$-0.076$	TD EPR	35
GaP:Cr $^{2+}$	1.97	2.03	$-1.5(1)^*$	$0.0657^*$	$0^*$	TD EPR	36
GaP:Mn $^{3+}$	2.00(5)	2.00(5)	$-1.141(5)^*$	$0.024(5)^*$	$0^*$	EPR/ TD EPR	This paper

occur for that transition in the high-field region. Because certain experimental data exist only for the high-field transitions, the spin-Hamiltonian parameters could not be determined independently. A coincidence with experimental data was achieved under the assumption of isotropic  $g$  values near 2 and  $F=0$ . The other  $d^4$  examples in III-V materials (Table I) confirm that for the ground state the orbital angular momentum is nearly completely quenched, yielding  $g$  values of about 2. Furthermore,  $F$  values substantially larger than  $a$  are not expected. The sign of the zero-field-splitting parameter  $D$  was found to be negative from the temperature dependence of the intensity of the high-field conventional EPR

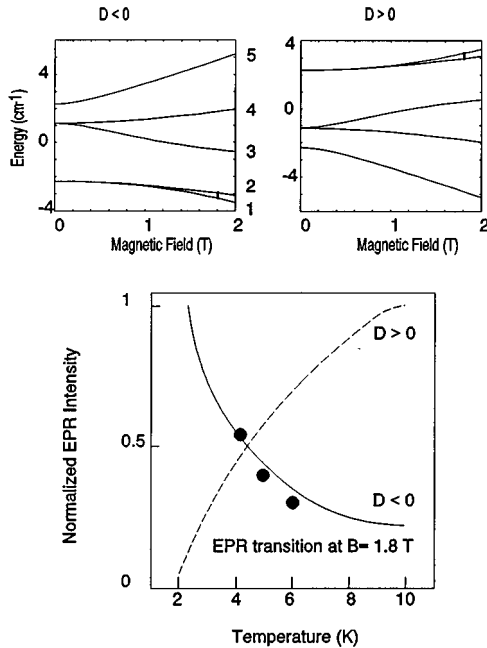


FIG. 9. Determination of the sign of the zero-field splitting parameter  $D$  of the  $\text{Mn}_{\text{Ga}}^{3+}(A^0)$  charge state in GaP from the investigation of EPR line intensities. The figure presents energy level diagrams assuming a positive sign and a negative sign of  $D$  at  $B \perp z$ . A comparison between the experimental data from conventional EPR experiments given by solid circles and the calculated temperature dependence of the line intensities (solid line for negative  $D$ , and dashed line for positive  $D$ ) shows that  $D$  is negative (bottom). The transition which has been analyzed is indicated in the level diagrams.

signals at about 1.8 T in the temperature range between 4 and 6 K (Fig. 9).

In both conventional and TD EPR, the spectral dependence of the Mn-related line intensities shows the conversion of  $\text{Mn}_{\text{Ga}}^{2+}(A^-)$  into  $\text{Mn}_{\text{Ga}}^{3+}(A^0)$  with an onset at  $h\nu_{\text{exc}} \approx 1.2$  eV (Fig. 10). The decrease of the  $\text{Mn}_{\text{Ga}}^{2+}(A^-)$  spectrum achieves saturation values of 60% ( $E1$ ) and 35% ( $A1$ ) of the dark values with the illumination conditions prevailing in our conventional EPR experiments. Therefore, the maximum achievable concentration of  $\text{Mn}_{\text{Ga}}^{3+}(A^0)$  is derived from the photo-EPR results to be  $[\text{Mn}^{3+}](E1) \approx 3.6 \times 10^{16} \text{ cm}^{-3}$  and  $[\text{Mn}^{3+}](A1) \approx 1.3 \times 10^{16} \text{ cm}^{-3}$ . In the case of conventional EPR, for  $h\nu_{\text{exc}} > 1.2$  eV, the  $\text{Fe}_{\text{Ga}}^{3+}(A^0)$  spectrum is also measured. The appearance and increase of  $\text{Fe}_{\text{Ga}}^{3+}(A^0)$  above  $h\nu_{\text{exc}} = 1.2$  eV is connected with a corresponding decrease of the  ${}^5E \rightarrow {}^5T_2$  absorption lines of  $\text{Fe}_{\text{Ga}}^{2+}(A^-)$  (Ref. 38) measured by optical absorption. The increase of  $\text{Fe}_{\text{Ga}}^{3+}(A^0)$  is caused by the capture of hole $_{\text{vb}}$  created according to Eq. (3) by  $\text{Fe}_{\text{Ga}}^{2+}(A^-)$ .

## VI. CONCLUSION

We have observed a photostimulated EPR spectrum in both conventional and TD EPR which could be attributed to the neutral Mn acceptor state  $\text{Mn}_{\text{Ga}}^{3+}(A^0)$ . This conclusion is supported by several arguments. First, the signal is Mn-

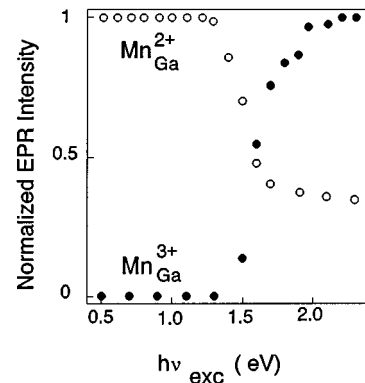


FIG. 10. Dependence of the photoinduced changes of the Mn-related conventional EPR signal intensities on illumination energy  $h\nu_{\text{exc}}$  of GaP:Mn A1 measured at  $T=20$  K. Open circles:  $\text{Mn}_{\text{Ga}}^{2+}(A^-)$ . Solid circles:  $\text{Mn}_{\text{Ga}}^{3+}(A^0)$ . The values at  $h\nu_{\text{exc}}=0.5$  eV are also the dark values.

related because the large linewidth indicates the unresolved  $^{55}\text{Mn}$  hyperfine splitting, and, second, the photostimulation of this signal is connected with a simultaneous decrease of the  $\text{Mn}_{\text{Ga}}^{2+}(A^-)$  signal. The latter verifies a direct conversion process for the Mn acceptor. Furthermore, the onset at 1.2 eV and the spectral dependence observed for the EPR signal coincide with that of the photoionization band of  $\text{Mn}_{\text{Ga}}^{3+}(A^0)$  in the optical-absorption experiments (cf. Figs. 2 and 10). Third, the angular dependencies have been argued to be determined by the general feature of a  $3d^4$  center on a tetrahedrally coordinated lattice site. They can be described by an  $S=2$  spin manifold in a tetragonal symmetry. The tetragonal distortion is caused by the action of a strain-stabilized  $T \otimes \epsilon$  Jahn-Teller effect, as has been reported previously for  $\text{Cr}^{2+}$  in several III-V materials (see Table I). *A priori*, we cannot exclude the possibility that the tetragonal distortion is produced by an associated defect, but complex model is very unlikely because it cannot explain the rapid

decrease in the signal intensity above 7 K and also because a  $\langle 100 \rangle$  distortion axis is not probable in that kind of as-grown tetrahedral host.

We have not found any signals with  $g$  values which are predicted for the neutral Mn acceptor state corresponding to  $\text{Mn}_{\text{Ga}}^{2+}$  and a delocalized hole<sup>1-3</sup> in the GaP:Mn samples. Therefore, we conclude that, in contrast to GaAs:Mn, in GaP:Mn the neutral acceptor state is a  $\text{Mn}_{\text{Ga}}^{3+}$  ion on strain-stabilized sites of tetragonal symmetry due to a strong Jahn-Teller coupling of the  $^5T_2$  ground state.

## ACKNOWLEDGMENTS

The authors would like to thank C. A. Bates, B. Clerjaud, and W. Gehlhoff for valuable discussions, and H. von Kiedrowski for the preparation of the oriented samples.

- 
- <sup>1</sup>J. Schneider, U. Kaufmann, W. Wilkening, M. Baumler, and F. Köhl, *Phys. Rev. Lett.* **59**, 240 (1987).
- <sup>2</sup>V. F. Masterov, K. F. Shtelmakh, and M. N. Barbashov, *Fiz. Tekh. Poluprovodn.* **22**, 654 (1988) [*Sov. Phys. Semicond.* **22**, 408 (1988)].
- <sup>3</sup>N. S. Averkiev, A. A. Gutkin, O. G. Krasikova, E. B. Osipov, and M. A. Reshchikov, *Fiz. Tekh. Poluprovodn.* **23**, 73 (1989) [*Sov. Phys. Semicond.* **23**, 44 (1989)].
- <sup>4</sup>M. Baumler, B. K. Meyer, U. Kaufmann, and J. Schneider, *Mater. Sci. Forum* **38-41**, 797 (1989).
- <sup>5</sup>Th. Frey, M. Maier, J. Schneider, and M. Gehrke, *J. Phys. C* **21**, 5539 (1988).
- <sup>6</sup>D. G. Andrianov, Yu. N. Bolsheva, G. V. Lazareva, A. S. Savelev, and S. M. Yakubeny, *Fiz. Tekh. Poluprovodn.* **17**, 810 (1983) [*Sov. Phys. Semicond.* **17**, 506 (1983)].
- <sup>7</sup>D. G. Andrianov, Yu. A. Grigorev, S. O. Klimonskii, A. S. Savelev, and S. M. Yakubeny, *Fiz. Tekh. Poluprovodn.* **18**, 262 (1984) [*Sov. Phys. Semicond.* **18**, 162 (1984)].
- <sup>8</sup>R. A. Chapman and W. G. Hutchinson, *Phys. Rev. Lett.* **18**, 443, 822(E) (1967).
- <sup>9</sup>M. Kleverman, E. Janzen, M. Linnarsson, and B. Monemar, in *Impurities, Defects and Diffusion in Semiconductors: Bulk and Layered Structures*, edited by D. J. Wolford, J. Pernholc, and E. E. Muller, MRS Symposia Proceedings No. 163 [Materials Research Society, Pittsburgh, 1990], p. 207.
- <sup>10</sup>M. Kleverman, E. Janzen, A. Thilderkvist, M. Linnarsson, and B. Monemar, in *Proceedings of the 21st International Conference on the Physics of Semiconductors*, edited by P. Jiang and H. Zheng (World Scientific, Singapore, 1992), p. 1657.
- <sup>11</sup>B. Lambert, B. Clerjaud, C. Naud, B. Deveaud, G. Picoli, and Y. Toudic, *J. Electron. Mater.* **14a**, 1141 (1985).
- <sup>12</sup>B. Plot-Chan, B. Deveaud, A. Rupert, and B. Lambert, *J. Phys. C* **19**, 5651 (1985).
- <sup>13</sup>V. F. Masterov, Yu. V. Maltsev, and K. K. Sobolevskii, *Fiz. Tekh. Poluprovodn.* **15**, 2127 (1981) [*Sov. Phys. Semicond.* **15**, 1235 (1981)].
- <sup>14</sup>Y. Dawei, B. C. Cavenett, and M. S. Skolnick, *J. Phys. C* **16**, L 647 (1983).
- <sup>15</sup>H. J. Sun, R. E. Peale, and G. D. Watkins, *Phys. Rev. B* **45**, 8310 (1992).
- <sup>16</sup>D. G. Andrianov, A. S. Savelev, and S. M. Yakubeny, *Fiz. Tekh. Poluprovodn.* **20**, 1253 (1986) [*Sov. Phys. Semicond.* **20**, 791 (1986)].
- <sup>17</sup>S. A. Abagyan, G. A. Ivanov, G. A. Koroleva, Yu. N. Kusnetsov, and Yu. A. Okunev, *Fiz. Tekh. Poluprovodn.* **9**, 369 (1975) [*Sov. Phys. Semicond.* **9**, 243 (1975)].
- <sup>18</sup>A. O. Ewvaraye and H. H. Woodbury, *J. Appl. Phys.* **47**, 1595 (1976).
- <sup>19</sup>R. F. Brunwin, B. Hamilton, J. Hodgkinson, A. R. Parker, and P. J. Dean, *Solid-State Electron.* **24**, 249 (1981).
- <sup>20</sup>R. S. Title and T. S. Plaskett, *Appl. Phys. Lett.* **14**, 76 (1969).
- <sup>21</sup>P. van Engelen and S. G. Sie, *Solid State Commun.* **30**, 515 (1979).
- <sup>22</sup>P. van Engelen, *Phys. Rev. B* **22**, 3144 (1980).
- <sup>23</sup>V. I. Kirilov, N. V. Pribylov, S. I. Rembeza, A. I. Spirin, and V. V. Teslenko, *Fiz. Tverd. Tela (Leningrad)* **24**, 1494 (1982) [*Sov. Phys. Solid State* **24**, 853 (1982)].
- <sup>24</sup>A. T. Vink and G. G. van Gorkom, *J. Lumin.* **5**, 379 (1972).
- <sup>25</sup>P. Omling and B. K. Meyer, *Phys. Rev. B* **44**, 5518 (1991).
- <sup>26</sup>G. Hofmann, F. G. Anderson, and J. Weber, *Phys. Rev. B* **43**, 9711 (1991).
- <sup>27</sup>G. Hofmann, A. Keckes, and J. Weber, *Semicond. Sci. Technol.* **8**, 1523 (1993).
- <sup>28</sup>S. J. C. H. M. van Gisbergen, M. Godlewski, T. Gregorkiewicz, and C. A. J. Ammerlaan, *Phys. Rev. B* **44**, 3012 (1991).
- <sup>29</sup>M. Feege, S. Greulich-Weber, and J.-M. Spaeth, *Semicond. Sci. Technol.* **8**, 1620 (1993).
- <sup>30</sup>In the  $Q$  band we have observed  $\text{Mn}^{2+}$  EPR spectra with identical  $g$  values and hyperfine constants in several materials.
- <sup>31</sup>H. Ch. Alt, R. Treichler, and J. Voelkl, *Appl. Phys. Lett.* **59**, 3651 (1991).
- <sup>32</sup>A. Vasson, A.-M. Vasson, N. Tebbal, M. El-Metoui, and C. A. Bates, *J. Phys. D* **26**, 2231 (1993).
- <sup>33</sup>W. Ulrici and J. Kreissl, in *Proceedings of the 5th Conference on Semi-insulating III-V Materials, Malmö*, edited by G. Grossmann and L. Ledebø (Institute of Physics and Physical Society, London, 1988), p. 381.

- <sup>34</sup>C. A. Bates, M. Darcha, J. Handley, A. Vasson, and A.-M. Vasson, *Semicond. Sci. Technol.* **3**, 172 (1988).
- <sup>35</sup>J. Handley, C. A. Bates, A. Vasson, A.-M. Vasson, K. Ferdjani, and N. Tebbal, *Semicond. Sci. Technol.* **5**, 710 (1990).
- <sup>36</sup>A.-M. Vasson, A. Vasson, M. El-Metoui, A. Erramli, A. Gavaix, and C. A. Bates, *Mater. Sci. Forum* **143-147**, 833 (1994).
- <sup>37</sup>C. A. Bates and K. W. H. Stevens, *Rep. Prog. Phys.* **49**, 783 (1986).
- <sup>38</sup>G. Rückert, K. Pressel, A. Dörnen, K. Thonke, and W. Ulrici, *Phys. Rev. B* **46**, 13 207 (1992).
- <sup>39</sup>J. J. Krebs and G. H. Stauss, *Phys. Rev. B* **16**, 971 (1977).
- <sup>40</sup>G. H. Stauss, J. J. Krebs, and R. L. Henry, *Phys. Rev. B* **16**, 974 (1977).